J Incl Phenom Macrocycl Chem (2009) 65:317–327
DOI 10.1007/s10847-009-9585-y

ORIGINAL ARTICLE

Template synthesis and characterization of cobalt(II) complex nanoparticles entrapped in the zeolite-Y

Masoud Salavati-Niasari

Received: 6 December 2008 / Accepted: 16 April 2009 / Published online: 7 May 2009

Abstract Zeolite encapsulated complex nanoparticles "$[Co([18]py_2N_4)]^{2+}$, $[Co([20]py_2N_4)]^{2+}$, $[Co(Bzo_2[18]py_2N_4)]^{2+}$ or $[Co(Bzo_2[20]py_2N_4)]^{2+}$" were successfully prepared by the template synthesis of 2,6-diacetylpyridine with $[Co(N–N)_2]^{2+}$ (N–N = 1,2-diaminoethane, 1,3-diamine propane, 1,2-diaminobenzene, 1,3-diaminobenzene) within the zeolite-Y. These complex nanparticles were entrapped in the Y-zeolite by a two-step process in the liquid phase: (i) inclusion of a Co(II) precursor complex, $[Co(N–N)_2]^{2+}$@NaY, and (ii) template synthesis of the cobalt(II) precursor complex with the 2,6-diacetylpyridine. The new complex nanoparticles entrapped in the zeolite Y "$[Co([18]py_2N_4)]^{2+}$@NaY, $[Co([20]py_2N_4)]^{2+}$@NaY, $[Co(Bzo_2[18]py_2N_4)]^{2+}$@NaY, $[Co(Bzo_2[20]py_2N_4)]^{2+}$@NaY" were characterized by several techniques: chemical analysis and spectroscopic methods (FT-IR, UV/VIS, XPS, XRD, BET, DRS). Analysis of the data indicates that the cobalt(II) complex nanoparticles are encapsulated in the zeolite-Y and exhibit different property from those of the free complexes, which can arise from distortions caused by steric effects due to the presence of sodium cations, or from interactions with the zeolite matrix.

Keywords Complex nanoparticles · Hexaaza · Cobalt(II) · Zeolite encapsulation

M. Salavati-Niasari (✉)
Institute of Nano Science and Nano Technology, University of Kashan, P. O. Box 87317-51167, Kashan, Iran
e-mail: salavati@kashanu.ac.ir

M. Salavati-Niasari
Department of Chemistry, University of Kashan, P. O. Box 87317-51167, Kashan, Iran

Introduction

IUPAC classifies porous materials into three categories, (1) microporous with pores of less than 2 nm in diameter, (2) mesoporous having pores between 2 and 50 nm, and (3) macroporous with pores greater than 50 nm. The term nanoporous materials have been used for those porous materials with pore diameters of less than 100 nm. Many kinds of crystalline and amorphous nanoporous materials such as framework silicates and metal oxides, zeolites, pillared clays, nanoporous silicon, carbon nanotubes and related porous carbons have been described lately in the literature [1–4]. Nanoporous materials are exemplified by crystalline framework solids such as zeolites, whose crystal structure defines channels and cages, i.e. nanopores, of strictly regular dimensions. They can impart shape selectivity for both reactants and the products when involved in the chemical reactions and processes. The large internal surface area and void volumes with extremely narrow pore size distribution as well as functional centers homogeneously dispersed over the surface make nanoporous solids highly active materials. Over the last decade, there has been a dramatic increase in synthesis, characterization and application of novel nanoporous materials [5–32].

Zeolites, which represent the largest group of nanoporous materials, are crystalline inorganic polymers based on a three-dimensional arrangement of SiO_4 and AlO_4 tetrahedral connected through their oxygen atoms to form large negatively-charged lattices with Brønsted and Lewis acid sites. These negative charges are balanced by extra-framework alkali and/or alkali earth cations. The most known zeolites are silicalite-1, ZSM-5, zeolite Beta and zeolites X, Y, and A. The incorporation of small amounts of transition metals into zeolitic frameworks influences their properties and generates their redox activity. Zeolites

with their well–organised and regular system of nano-pores and nanocavities also represent almost ideal matrices for hosting nanosized particles e.g. transition metal complexes that can also be involved in catalytic applications.

In this paper, I report the synthesis and characterization of cobalt(II) complex nanoparticles of 18- and 20-membered hexaaza macrocyclic ligand; [18]py_2N_4: 3,6,14,17,23,24-hexaazatricyclo[17.3.1.1^{8,12}]tetracosa-1(23),2,6,8(24),9,11,13,17,19,21-decane; [20]py_2N_4: 3,7,15,19,25,26-hexaazatricyclo[19.3.1.1^{9,13}]hexacosa-1(25),2,7,9(26),10,12,14,19,21,23-decaene; Bzo_2[18]py_2N_4 : 3,10,18,25,31,32-hexaazapentacyclo[25.3.1.1.^{12,16}.0^{4,9}.0^{19,24}]dotriaconta 1(31),2,4(9),5,7,10,12(32),13,15,17,19,21,23,25,29-hexadecane; Bzo_2[18]py_2N_4: 2,10,16,24,30,32-hexaazapentacyclo[23.3.1.1^{4,8}.1^{1,1,15}1^{18,22}otriaconta-1(29),2,4,6,8(32),9,11,13,15(31),16,18(30),19,21,23,25,27-hexadecane; encapsulated within the zeolite-Y by the template condensation of 2,6-diacetylpyridine and $[Co(N\text{-}N)_2]^{2+}$; $[Co([18]py_2N_4)]^{2+}$@NaY, $[Co([20]py_2N_4)]^{2+}$@NaY, $[Co(Bzo_2[18]py_2N_4)]^{2+}$@NaY and $[Co(Bzo_2[20]py_2N_4)]^{2+}$@NaY; shown in Scheme 1, 2.

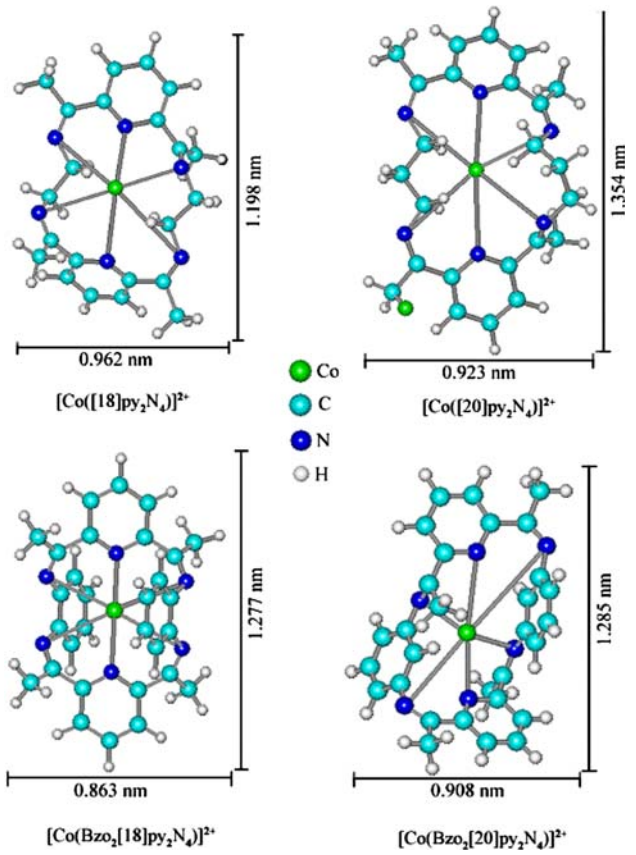

Scheme 1 18-, and 20-membered hexaaza macrocyclic cobalt(II) complexes

Experimental section

Materials and physical measurements

Safety note: Cobalt perchlorate salt with organic ligands is often explosive and should be handled with caution. All other reagents and solvents were purchased from Merck (pro-analysis) and dried using molecular sieves (Linde 4Å). Solvents was distilled under nitrogen and stored over molecular sieves (4Å). NaY with the Si:Al ratio of 2.53 was purchased from Aldrich (Lot No. 67812). The complex $[Co(N\text{-}N)_2](ClO_4)_2$ was prepared according to the published procedures [33]. Hexaaza macrocyclic ligands ([18]py_2N_4, [20]py_2N_4, Bzo_2[18]py_2N_4 and Bzo_2[20]-py_2N_4) were prepared by following the procedures reported in Ref. [34]. The elemental analysis (carbon, hydrogen and nitrogen) of the materials was obtained from Carlo ERBA Model EA 1108 analyzer. XRD patterns were recorded by a Rigaku D-max C III, X-ray diffractometer using Ni-filtered Cu Kα radiation. Nitrogen adsorption measurements were performed at 77 K using a Coulter Ofeisorb 100CX instrument. The samples were degassed at 150 °C until a vacuum better than 10^{-3} Pa was obtained. Micropore volumes were determined by the *t*-method, a "monolayer equivalent area" was calculated from the micropore volume [35, 36]. FAB mass spectra were recorded on a Kratos MS50TC spectrometer. FT-IR spectra were recorded on Shimadzu Varian 4300 spectrophotometer in KBr pellets. The electronic spectra of the neat complexes were taken on a Shimadzu UV-Vis scanning spectrometer (Model 2101 PC). The stability of the encapsulated catalyst was checked after the reaction by UV-Vis and possible leaching of the complex was investigated by UV-Vis in the reaction solution after filtration of the zeolite. The amounts of complex nanoparticles encapsulated in zeolite matrix were determined by the elemental analysis and by subtracting the amount of metallocomplex left in the solutions after the synthesis of the catalysts as determined by UV-Vis spectroscopy, from the amount taken for the synthesis. Atomic absorption spectra (AAS) were recorded on a Perkin-Elmer 4100–1319 Spectrophotometer using a flame approach, after acid (HF) dissolution of known amounts of the zeolitic material and SiO_2 was determined by gravimetric analysis. Diffuse reflectance spectra (DRS) were registered on a Shimadzu UV/3101 PC spectrophotometer the range 1500–200 nm, using MgO as reference. XPS (small area X-ray photoelectron spectroscopy) data were recorded with the PHI–5702 Multi-Technique System, Power Source by Mg Kα line and Ag 3d5/2 FWHM 6 0.48 eV. Thermogravimetric-differential thermal analysis (TG-DTA) were carried out using a thermal gravimetric analysis instrument (Shimadzu TGA-50H) with a flow rate of 20.0 mL min^{-1} and a heating rate of 10 °C min^{-1}.

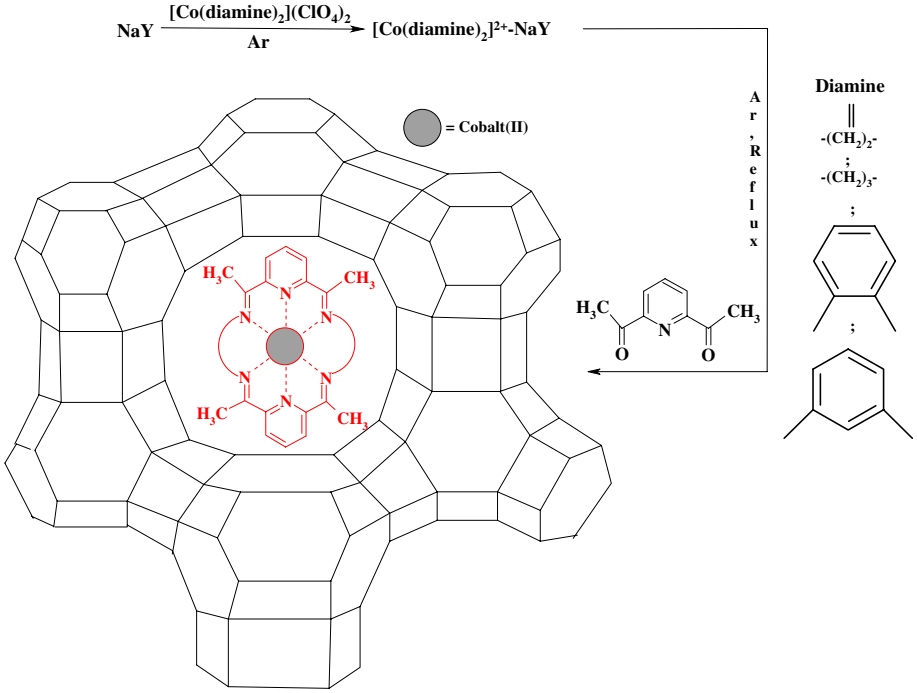

Scheme 2 Encapsulation cobalt(II) complex nanoparticles of 18-, and 20-membered hexaaza macrocyclic within the zeolite-Y

Preparation of $[Co([18]py_2N_4)]^{2+}$, $[Co([20]py_2N_4)]^{2+}$, $[Co(Bzo_2[18]py_2N_4)]^{2+}$ and $[Co(Bzo_2[20]py_2N_4)]^{2+}$

To a stirred methanol solution (500 mL) of $[Co(diamine)_2](ClO_4)_2$ (42.07 mmole; diamine = 1,2-diaminoethane (2.53 g), 1,3-diaminopropane (3.11 g), 1,2-diaminobenzene (4.54 g) or 1,3-diaminobenzene (4.54 g)) were slowly added 2,6-diacetylpyridine (13.69 g, 84.20 mmole) under nitrogen atmosphere. The mixture was heated at reflux for 12 h until a dark red solution resulted. The solution was cooled to room temperature and filtered to remove cobalt hydroxide. Excess perchloric acid or lithium perchlorate dissolved in methanol was added to the filtrate, and the mixture was kept in the refrigerator until red solid formed. The red solid were filtered, washed with diethyl ether, and air-dried. The products were crystallized from hot methanol.

Preparation of Co(II)@NaY

An amount of 2 g NaY zeolite was suspended in 100 ml distilled water, which contained $Co(NO_3)_2.6H_2O$ (0.025 M). The mixture was then heated while stirring at 90 °C for 24 h. The light pink solid was filtered, washed with hot distilled water till the filtrate became free from any cobalt(II) ion (by AAS of filtrate) content and dried for 10 h at 80 °C under vacuum. The ionic exchange degree was determined by AAS.

Preparation of $[Co(N\text{-}N)_2]^{2+}$@NaY

Typically a 4 g sample of NaY zeolite was mixed with 0.37 g of $[Co(N\text{-}N)_2](ClO_4)_2$; diamine = 1,2-diaminoethane, 1,3-diaminopropane, 1,2-diaminobenzene or 1,3-diaminobenzene; suspended in 100 ml of MeOH and then refluxed for 8 h. The pale orange solid consisting of $[Co(N\text{-}N)_2]^{2+}$ exchanged with Na^+ in NaY and denoted as $[Co(N\text{-}N)_2]^{2+}$@NaY, was collected by filtration, washed with ethanol. The resulted zeolites, were Soxhlet extracted with ethanol (for 4 h) and then with chloroform (for 3 h) to remove excess unreacted diamine and any Co(II) complexes adsorbed onto the external surface of the zeolite crystallines. The resulting light orange solids were dried at 60 °C under vacuum for 24 h.

Preparation of complex nanoparticles entrapped in the zeolite Y

To a stirred methanol suspension (100 mL) of $[Co(N\text{–}N)_2]^{2+}$@NaY (2 g) were slowly added 2,6-diacetylpyridine (under N_2 atmosphere). The mixture was heated under reflux condition for 24 h until a pale red suspension resulted. The solution was filtered and the resulting zeolites, were Soxhlet extracted with chloroform (for 4 h) and then with ethanol (for 4 h) to remove excess unreacted products from amine-ketone condensation and any cobalt(II) complexes adsorbed onto the external surface of the zeolite crystallites. The resulting pale red solids were dried

at 70 °C under vacuum for 12 h. The remaining [bis(diamine)cobalt(II)] ions in zeolite were removed by exchanging with aqueous 0.1 M NaCl solutions. The stability of the encapsulated complex nanoparticles was checked after the reaction by UV-Vis and possible leaching of the complex was investigated by UV-Vis in the reaction solution after filtration of the zeolite. The amounts of Co(II) complexes encapsulated in zeolite matrix were determined by the elemental analysis and by subtracting the amount of Co(II) complex left in the solutions after the synthesis of the materials as determined by UV-Vis spectroscopy, from the amount taken for the synthesis.

Results and discussion

Cobalt(II) complexes were prepared by reacting 2 equiv of 2,6-diacetylpyridine and 1 equiv of $[Co(N\text{-}N)_2]^{2+}$ (Scheme 1). The complexes are soluble in dimethylformamide (DMF) and dimethylsulfoxide (DMSO), but are insoluble in common organic solvents and water. They are thermally stable up to ~250 °C. The complexes are extremely stable in the solid state and in solution and are relatively stable against ligand dissociation even in highly acidic solutions. The analytical data of the metal chelates are given in Table 1, which show that chelates may be represented by the formula $[Co([18]py_2N_4)](ClO_4)_2$, $[Co([20]py_2N_4)](ClO_4)_2$, $[Co(Bzo_2[18]py_2N_4)](ClO_4)_2$ and $[Con(Bzo_2[20]py_2N_4)](ClO_4)_2$.

The measurements of molar conductance in DMF show that these chelates are 1:2 electrolytes. The tests for anions are positive directly without decomposing the chelates showing their presence outside the coordination sphere. The molecular formula of the complexes has been assigned on the basis of the results of their elemental analyses and the molecular ion peaks in the mass spectra (Table 1).

Synthesis of cobalt(II) complex nanoparticles encapsulated in the zeolite-Y involves two steps: (i) exchange of $[Co(N\text{–}N)_2]^{2+}$ (N–N = 1,2-diaminoethane, 1,3-diaminopropane, 1,2-diaminobenzene or 1,3-diaminobenzene) ions with NaY in methanol solution and (ii) reaction of $[Co(N\text{–}N)_2]^{2+}$@NaY with excess 2,6-diacetylpyridine in methanol where 2,6-diacetylpyridine slowly enters into the nanocavity of zeolite-Y due to its template nature and interacts with $[Co(N\text{–}N)_2]^{2+}$ ions. Soxhlet extraction using ethanol and chloroform finally purified the impure complexes. The remaining uncomplexed metal ions in zeolite were removed by exchanging with aqueous 0.01 M NaCl solution. As one extra anionic ligand would be required to balance the overall charges on the Co(II), Cl^- of NaCl used during exchanged process fulfills this requirement. Thus, the formula of cobalt(II) complex may be written as $[Co([18]py_2N_4)]^{2+}$@NaY, $[Co([20]py_2N_4)]^{2+}$@NaY, $[Co(Bzo_2[18]py_2N_4)]^{2+}$@NaY, $[Co(Bzo_2[20]py_2N_4)]^{2+}$@NaY.

The percentage of metal contents determined before and after encapsulation by inductively coupled plasma (ICP) along with their expected formula is presented in Table 2. As crude mass was extracted with methanol, the metal ion content found after encapsulation is only due to the presence of metal complexes in the nanopores of the zeolite-Y. The molecular formula of the complex nanoparticles are based on the neat complexes $[Co([18]py_2N_4)]^{2+}$, $[Co([20]py_2N_4)]^{2+}$, $[Co(Bzo_2[18]py_2N_4)]^{2+}$ and $[Co(Bzo_2[20]\text{-}py_2N_4)]^{2+}$ that have also been prepared and characterized.

The flexible ligand synthesis scheme leads to the encapsulation of Co(II) complex nanoparticles of macrocyclic ligands inside the nanopores of zeolite. The results of chemical analysis of the samples are given in Table 2. The parent NaY zeolite has Si/Al molar ratio of 2.53 which corresponds to a unit cell formula $Na_{56}[(AlO_2)_{56}(SiO_2)_{136}]$. The unit cell formula of metal-exchanged zeolites shows 11 moles of cobalt dispersion per unit cell ($Na_{34}Co_{11}[(AlO_2)_{56}(SiO_2)_{136}].nH_2O$). Metal ion exchange at around 34% leads to 2.62–2.68% of metal loading in zeolite. The CHN analysis results of the neat cobalt complexes showed near similarity to the theoretical values. The cobalt contents of the zeolite encapsulated samples were estimated by dissolving known amounts of the catalyst in concentric HCl and using AAS. The analytical data of each complex indicate molar ratios of Co:C:H almost close to those calculated for the mononuclear structure (Table 2). However, the presence of minute traces of free metal ions in the lattice could be assumed as the metal content which is slightly higher than the stoichiometric requirement. Only a portion of metal ions in metal-exchanged zeolite has undergone complexation and the rest is expected to be removed on re-exchange with sodium nitrate solution. But, some of these cation sites in the zeolite lattice might be blocked from access solution by the encapsulated complexes. This shielding effect is more probable in the present case since the complex loading level is relatively higher than that reported previously [37]. The remaining trace amount of free metal ions in the zeolite doesn't show any serious interference in the behavior of the encapsulated complexes [38–40].

The Si and Al contents in the metal-exchanged zeolites and the zeolite complex nanoparticles are almost the same ratio as in the parent zeolite. This indicates little changes in the zeolite framework due to the absence of dealumination in metal ion exchange. The X-ray diffraction patterns of encapsulated complex nanoparticles are shown in Fig. 1. The encapsulated complexes exhibit similar peaks to those of NaY; except for a slight change in the intensity of the peaks, no new crystalline pattern emerges. These facts confirmed that the framework and crystallinity of zeolite

Table 1 Elemental analysis, vibrations parameters and some physical properties for ligands and 18- and 20-membered hexaaza macrocyclic cobalt(II) complexes

Complex	Calculated (Found)					Λ_M^a, Ω^{-1} cm^2 mol^{-1}	μ_{eff} (MB)	IR (KBr, cm^{-1})			d ↔ d (nm; ε, l mol^{-1} cm^{-1})	[Co–ClO_4]$^+$	[Co–2ClO_4 –H]$^+$
	%C	%H	%N	C/N	%Co			υ(C=N)	υ(py)	υ(ClO_4^{-1})			
[18 py_2N_4	70.56 (70.34)	7.00 (6.89)	22.44 (22.60)	3.14 (3.11)	–	–	–	1620	1590	–	–	–	–
[Co([18]py_2N_4)] (ClO_4)$_2$	41.79 (41.56)	4.14 (4.03)	13.29 (13.40)	3.14 (3.10)	9.32 (9.16)	340	3.90	1613	1592	1090, 624	1010 (64) 630 (85) 532 (98) 397 (120)	533	433
[20]py_2aneN_4	71.61 (71.42)	7.51 (7.40)	20.88 (21.00)	3.43 (3.40)	–	–	–	1618	1598	–	–	–	–
[Co([20]py_2N_4)] (ClO_4)	43.65 (43.49)	4.58 (4.43)	12.73 (12.87)	3.43 (3.38)	8.92 (8.80)	336	3.89	1610	1600	1093, 626	1013 (69) 633 (88) 534 (103) 398 (140)	561	461
Bzo_2[18]py_2N_4	76.57 (76.38)	5.57 (5.43)	17.86 (17.98)	4.29 (4.24)	–	–	–	1630	1601	–	–	–	–
[Co(Bzo_2[18] py_2N_4)](ClO_4)	49.47 (49.29)	3.60 (3.49)	11.54 (11.70)	4.29 (4.21)	8.09 (7.91)	332	3.92	1623	1602	1094, 623	1007 (63) 628 (82) 530 (95) 398 (117)	629	529
Bzo_2[20]py_2N_4	76.57 (76.40)	5.57 (5.45)	17.86 (17.90)	4.29 (4.27)	–	–	–	1635	1603	–	–	–	–
[Co(Bzo_2[20] py_2N_4)](ClO_4)	49.47 (49.30)	3.60 (3.52)	11.54 (11.68)	4.29 (4.22)	8.09 (7.88)	330	3.91	1630	1603	1091, 622	1011 (68) 626 (89) 535 (100) 399 (135)	629	529

[a] In DMF solutions

Table 2 Chemical composition, d ↔ d transition and IR stretching frequencies (as KBr pellets) of 18- and 20-membered hexaaza macrocyclic cobalt(II) complex nanoparticles encapsulated in the zeolite Y

Sample	C (%)	H (%)	N (%)	C/N	Si (%)	Al (%)	Na (%)	Co (%)	Si/Al	$\upsilon_{C=N}$ (cm^{-1})	d ↔ d (nm)
NaY	–	–	–	–	21.76	8.60	7.50	–	2.53	–	–
Co(II)@NaY	–	–	–	–	22.08	8.73	3.34	3.71	2.53	–	–
$[Co([18]py_2N_4)]^{2+}$@NaY	4.82	1.75	1.60	3.03	20.80	8.22	5.27	2.68	2.53	1615	1008, 628, 530, 397
$[Co([20]py_2N_4)]^{2+}$@NaY	4.80	1.80	1.50	3.20	20.75	8.20	5.25	2.65	2.53	1613	1011, 631, 533, 397
$[Co(Bzo_2[18]py_2N_4)]^{2+}$@NaY	4.84	1.83	1.19	4.08	20.70	8.18	5.20	2.62	2.53	1625	1005, 626, 531, 398
$[Co(Bzo_2[20]py_2N_4)]^{2+}$@NaY	4.85	1.82	1.18	4.10	20.72	8.19	5.22	2.63	2.53	1628	1010, 625, 533, 398

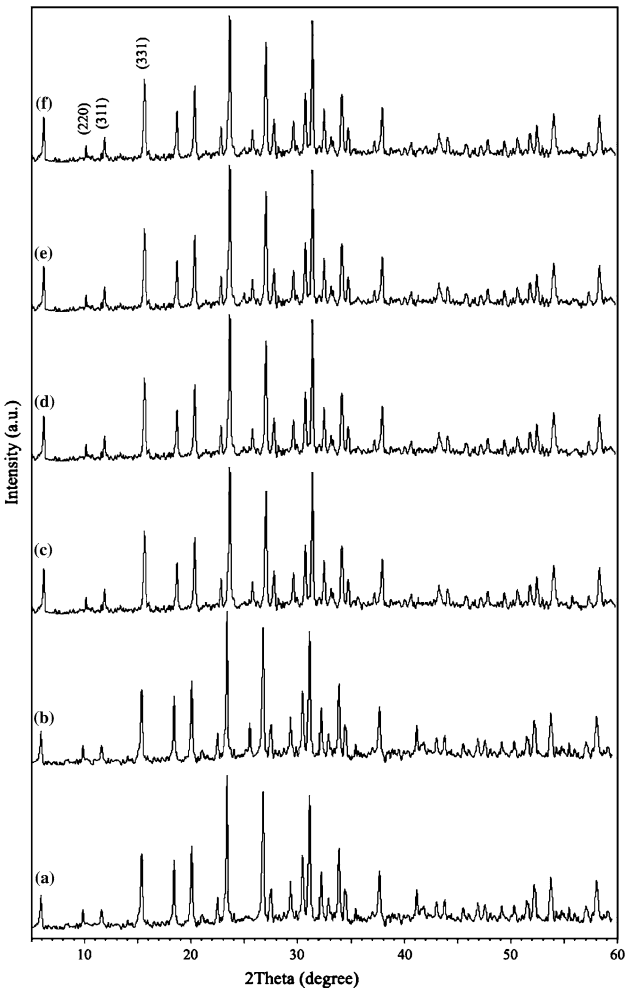

Fig. 1 XRD patterns of (**a**) NaY, (**b**) Co@NaY, (**c**) $[Co([18]py_2N_4)]$@NaY, (**d**) $[Co([20]py_2N_4)]$@NaY, (**e**) $[Co(Bzo_2[18]py_2N_4)]$@NaY and (**f**) $[Co(Bzo_2[20]py_2N_4)]$@NaY

were not destroyed during the preparation, and that the complexes were well distributed in the cages. The relative peak intensities of the 220, 311 and 331 reflections have been thought to be correlated to the locations of cations. In NaY, the order of peak intensity is in the order: 331 > 220 > 311, while in encapsulated complexes, the order of peak intensity became 331 > 311 > 220. The difference indicates that the ion-exchanged Co^{2+}, which substitutes at the location of Na^+, undergoes rearrangement during complexation [41].

The TGA profile of one of the representative encapsulated cobalt(II) complex nanoparticles, $[Co([18]py_2N_4)]^{2+}$@NaY is given in Fig. 2. The thermal decomposition of all these materials occurs in two steps. First step starts shortly after increasing the temperature above 150 °C and continues until the loss of all intrazeolite water. Second step occurs in a wide temperature range (300–700 °C) and is due to the slow decomposition of the chelating ligand. A very small weight percentage loss indicates the presence of only small amount of metal complex insertion in the nanocavity of the zeolite. This is in agreement with the low percentage of metal content estimated by atomic absorption spectrometer. Compared to the neat complex, the decomposition of the zeolite-encapsulated complex nanoparticles occurs at the higher temperature. A similar enhancement of the thermal stability of a metal complex on encapsulation has been observed earlier [42].

The surface area and pore volume of the materials is presented in Table 3. The encapsulation of $[Co([18]py_2N_4)]^{2+}$, $[C0([20]py_2N_4)]^{2+}$, $[Co(Bzo_2[18]py_2N_4)]^{2+}$ and $[Co(Bzo_2[20]py_2N_4)]^{2+}$ complexes in zeolite reduced the adsorption capacity and the surface area of the zeolite. The lowering of the pore volume and surface area indicated the presence of complexes ($[Co([18]py_2N_4)]^{2+}$, $[Co([20]py_2N_4)]^{2+}$, $[Co(Bzo_2[18]py_2N_4)]^{2+}$, $[Co(Bzo_2[20]py_2N_4)]^{2+}$) within the zeolite nanocages and not on the external surface.

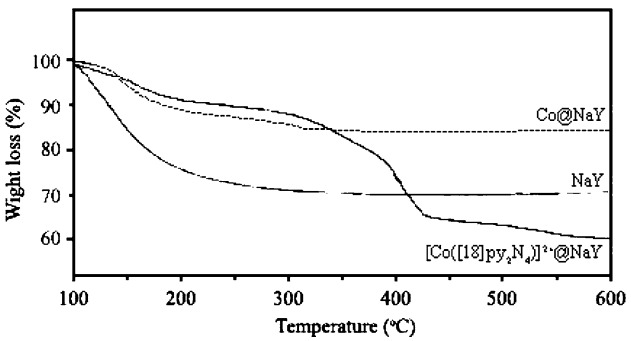

Fig. 2 TGA profiles of NaY, Co@NaY and $[Co([18]py_2N_4)]$@NaY

Table 3 Surface area and pore volume data of 18- and 20-membered hexaaza macrocyclic cobalt(II) complex nanoparticles encapsulated in zeolite Y

Sample	Surface area[a] (m^2/g)	Pore volume[b] (ml/g)
NaY	545	0.31
Co(II)@NaY	532	0.30
$[Co([18]py_2N_4)]^{2+}$@NaY	320	0.11
$[Co([20]py_2N_4)]^{2+}$@NaY	315	0.10
$[Co(Bzo_2[18]py_2N_4)]^{2+}$@NaY	286	0.08
$[Co(Bzo_2[20]py_2N_4)]^{2+}$@NaY	277	0.07

[a] Surface area is the "monolayer equivalent area" calculated as explained in the reference 20, 21

[b] Calculated by the *t*-method

The IR spectra of all the complexes do not exhibit any bands in the region at *ca* 3400–3200 cm^{-1}, the characteristic frequency of the free–NH_2 group. There is no absorption ~1600–1700 cm^{-1} due to the free carbonyl group [43]. The absence of stretching and bending vibrations of the (C-O) group at *ca* 1525 and 1280 cm^{-1} substantiate the absence of this group [44]. The strong bands appearing as doubles at *ca* 1610–1640 cm^{-1} may be assigned to υ(C=N) vibrations and point towards the coordinated azomethine groups [45, 46]. Therefore, it is clear from the IR spectra that both the NH_2 groups of diamine have condensed with both the carbonyl groups of 2,6-diacetylpyridine to give rise to an N_6 arrangement of four azomethine and two pyridine nitrogen atoms equally suitable for coordination. 2,6-Disubstituted pyridine derivatives show various bands at *ca* 1585–1615, 1570–1590, 1455–1490 and at *ca* 1440–1445 cm^{-1} can be assigned to four υ(C=C) skeletal frequencies and designated as bands I, II, III and IV of pyridine rings, respectively [47]. In the spectra of complexes under study, a strong band at *ca* 1615 cm^{-1} with a shoulder at *ca* 1610 cm^{-1} may be assigned to symmetric and anti-symmetric stretching modes of the azomethine linkage [48] and the frequency concerned with the $\upsilon_{(C=N)}$ stretching mode shifted to lower range by 2–5 cm^{-1}, with a marginal loss of the intensity of the band. This lowering may be taken as an indication of the coordination of the nitrogen of the azomethine group to the metal atom [49]. The appearance of one band at *ca* 1080 and 625 cm^{-1} assignable to ClO_4^- stretching and bending modes, respectively, are found in the perchlorato complexes of cobalt(II). The position of these bands is compatible with the ionic perchlorate group [50]. The far-IR spectra of the complexes show various bands in various regions assignable to pyridine ring and metal-nitrogen vibrations. The spectra of the complexes derived from 2,6-diacetylpyridine and diamine show bands at ca 415 and 600 cm^{-1}, assignable to (C–C) out-of-plane and (C–C) in-plane deformations. The vibrations suffer significant shift towards higher frequencies and support pyridine-nitrogen coordination to the metal atom [51]. The spectra also exhibit various bands in the region at *ca* 260–280 cm^{-1}. In this region the various vibrations observed are at ca 260–270, 265–274 and 275–280 cm^{-1} and these may be assigned to υ(Co-py) stretching vibrations, respectively [52]. The far-IR spectra also show various bands at ca ~455 cm^{-1}, which implies $\upsilon_{(Co-N)}$ (azomethine) vibrational modes and confirms the involvement of the azomethine nitrogen.

IR spectroscopy provided information on the integrity of the encapsulated complex nanoparticles, as well as the crystallinity of the host zeolite. The IR bands of all encapsulated complexes were weak due to their low concentration in the zeolite. Co(II) complexes encapsulated in the zeolite cages did not show any significant shift in C=N stretching modes. We did not notice any appreciable changes in the frequencies of Co complexes after incorporation into zeolite matrix. The major FT-IR bands of the encapsulated complexes are tabulated in Table 2. All metal complexes encapsulated zeolites exhibit band around 1140, 1035, 960, 780 and 740 cm^{-1} due to zeolite framework. No significant broadening or shift of the structure-sensitive zeolite vibrations at 1130 cm^{-1} (due to the asymmetric T–O stretch) on encapsulation of metal complexes indicates that there is no significant expansion of the zeolite nanocavities or dealumination during the encapsulation process. This further indicates that, the structure of metal complexes fit nicely within the cavity of the zeolite.

At room temperature the magnetic moment measurements of the cobalt(II) complexes lie in the range ~3.90 BM corresponding to three unpaired electrons, Table 1. The electronic spectra of all the cobalt(II) complexes, Table 1, exhibits absorption in the region ~1010 nm ($\varepsilon = 64$ mol^{-1} cm^{-1}), ~630 nm ($\varepsilon = 85$ l mol^{-1} cm^{-1}), ~532 nm ($\varepsilon = 98$ l mol^{-1} cm^{-1}) and ~395 nm ($\varepsilon = 120$ l mol^{-1} cm^{-1}). These bands may be assigned to the following transitions: $^4T_{1g}(F) \rightarrow {}^4T_{2g}(F)$, $^4T_{1g} \rightarrow {}^4A_{2g}$ and $^4T_{1g}(F) \rightarrow {}^4T_{1g}(P)$, respectively. The fourth band may be due to charge transfer. The position of bands indicates that these complexes have distorted octahedral geometry [53–57], Scheme 1, and might possess D_{4h} symmetry. When the complex nanoparticles were encapsulated in zeolite-Y, the d↔d band shifted again to the higher energy side. The stability of the complexes increases apparently when they are encapsulated in zeolite-Y. The position of the d↔d band corresponds to a octahedral geometry for macrocyclic cobalt(II) complex nanoparticles.

The presence of the complex in NaY was supported by XPS analysis. All modified NaY samples revealed the presence of oxygen, sodium, silicon and aluminium from the zeolite lattice in their XPS resolution spectra. The

Table 4 Curve fitting data of the XPS spectra in the Si 2p, Al 2p, Na 1s, Co 2p3/2, C 1s, O 1s and N 1s bands of the samples

	Binding energy (eV)								
	Si (2p)	Al (2p)	Na (1s)	Co (2p3/2)	C (1s)	O (1s)	N (1s)	Si/Al[a]	2p3/2 and 2p1/2 separation (eV)
NaY	103.5	75.1	1072.6	–	285.0	531.0	–	2.62	–
Co(II)@NaY	103.5	75.1	1072.6	780.2	285.0	532.5	–	2.58	–
$[Co([18]py_2aneN_4)]^{2+}$@NaY	103.5	75.1	1074.01	782.5	285.0, 286.5	532.6	400.2	2.41	15.8
					286.9, 289.4		402.4		
$[Co([20]py_2aneN_4)]^{2+}$@NaY	103.5	75.1	1074.	782.3	285.0, 286.5	532.6	400.2	2.42	15.6
					286.9 289.4		402.4		
$[Co(Bzo_2[18]py_2aneN_4)]^{2+}$@NaY	103.5	75.1	1074.2	782.7	285.0, 286.9	532.7	400.5	2.38	16.1
					289.5, 289.1		402.4		
$[Co(Bzo_2[20]py_2aneN_4)]^{2+}$@NaY	103.5	75.1	1074.2	782.6	285.0, 286.9	532.7	400.5	2.38	15.7
					289.5, 289.1		402.4		

[a] Amount of the elements determined by XPS analysis of the samples

bands typical of the Co(II)-py_2N_4 complex, scarcely visible because of their low loading, were identified in the Co $2p_{3/2}$ and N 1s region. The bulk (Table 1) and the surface Si/Al (Table 4) atomic ratios of NaY and of modified samples were similar, which indicates that dealumination does not occur during the encapsulation procedure. The binding energies of the elements detected by XPS are summarized in Table 4. The most intense bands identified are due to the zeolite structure, in the Si 2p region a band at 103.5 eV typical for Si atoms with different chemical environments, such as SiO_4 and terminal Si–OH groups. In the Al 2p region a band at 75.1 eV from the tetrahedral AlO_4 groups and a symmetrical large band at 531.0 eV from the O 1s region, and finally a band in the Na 1s region at 1072.6 eV were also observed (Table 4).

As appears from Table 4, the amount of surface cobalt is very similar to the bulk cobalt content (Table 1), which that suggests the Co(II)-py_2N_4 complexes are homogeneously distributed throughout the NaY crystals. The medium binding energy values for Co 2p3/2 are different before and after encapsulation, which indicates the change in environment of the cobalt upon coordination with the py_2N_4 ligand. Before coordination the medium binding energy of Co 2p3/2 value is 780.2 eV (Co(II)@NaY) and after the complex encapsulation the value is 782.5 eV, $[Co([18]py_2N_4)]^{2+}$@NaY; 782.3 eV, $[Co([20]py_2N_4)]^{2+}$@NaY; 782.7 eV, $[Co(Bzo_2[18]py_2N_4)]^{2+}$@NaY and 782.6 eV, $[Co(Bzo_2[20]py_2N_4)]^{2+}$@NaY (Table 4). These results confirm the same cobalt coordination sphere for the complex when free or encapsulated within NaY zeolite and that the host matrix environment does not affect the valence state of the metal atom of the complex.

Figure 3 shows the Co 2p core levels of neat and encapsulated complexes. Cobalt remains in the 2+ oxidation state in both the neat and encapsulated complexes and it matches well with the reported values for similar systems [58–60]. There is a strong increase in satellite intensity for Co 2p levels and a large energy gap (16.1–16.7 eV) between them is observed from encapsulated complex, which results in higher stability than neat complex. Table 4 lists the relevant parameters for Co complexes.

The high resolution C 1s spectrum of encapsulated complexes shows an asymmetric band centered at 285.0 eV that can be deconvoluted into three individual bands (Table 4). The three bands at high energy were also observed in the starting material and are presumably due to the presence of some contamination. The band at 289.0 eV is attributed to the aromatic carbons of the py_2N_4 ligand. The encapsulated complexes and the free complex samples exhibit in the N 1s region a band centred at 400.1 and 402.3 eV, due to the contribution of nitrogen atoms of the ligand (Fig. 3).

Conclusion

The hexaaza complex nanoparticles; $[Co([18]py_2N_4)]^{2+}$, $[Co([20]py_2N_4)]^{2+}$, $[Co(Bzo_2[18]py_2N_4)]^{2+}$ and $[Co(Bzo_2[20]py_2N_4)]^{2+}$; have been encapsulated in the nanocavity of zeolite by template condensation between preentrapped; [bis(diamine)cobalt(II)] (diamine = 1,2-diaminoethane, 1,3-diaminopropane, 1,2-diaminobenzene, 1,3-diaminobenzene), $[Co(N–N)_2]^{2+}$@NaY; complexes with 2,6-diacetylpyridine. This strategy appears to be effective for the encapsulated of Co(II) complexes with 18-, 20-membered hexaaza macrocycle ligands derived from $[Co(N–N)_2]^{2+}$@NaY, as template condensation in the

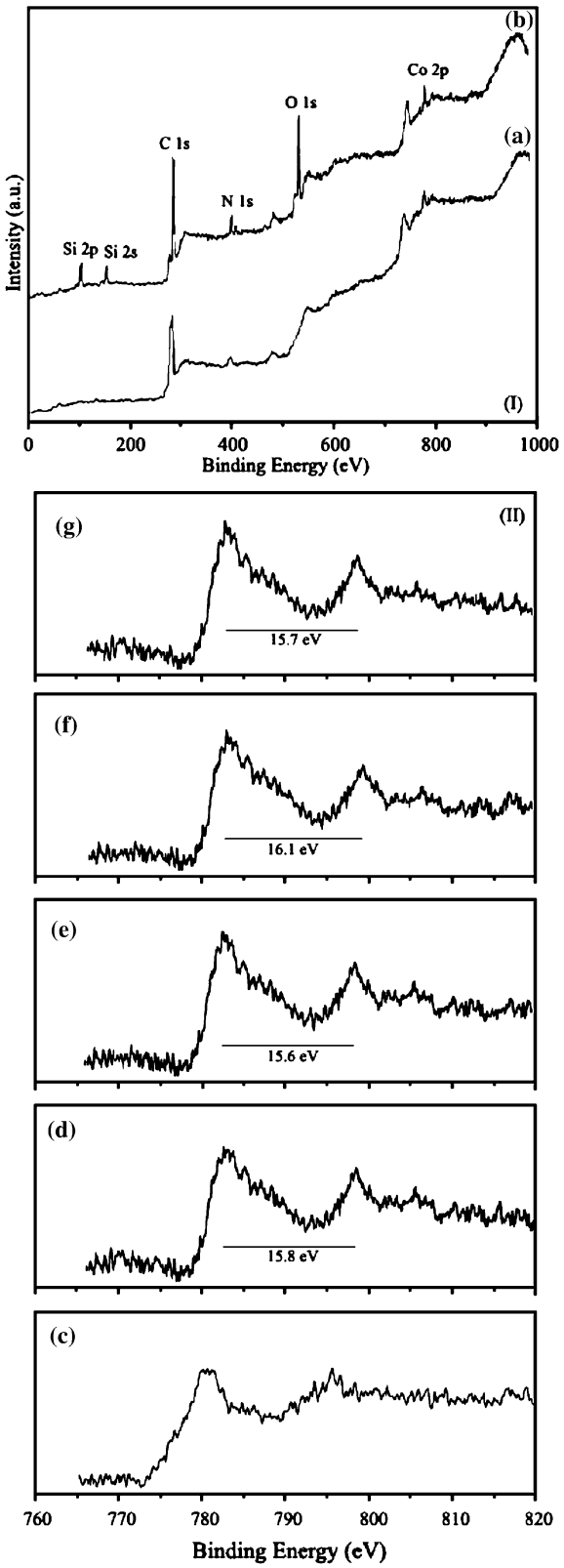

Fig. 3 XPS spectra of (I) (**a**), $[Co([18]py_2N_4)](ClO_4)_2$; (**b**), $[Co([18]py_2N_4)]$@NaY. (II) XPS Co 2p2/3 of (**c**), $[Co([18]py_2N_4)](ClO_4)_2$; (**d**), $[Co([18]py_2N_4)]$@NaY; (**e**), $[Co([20]py_2N_4)]$@NaY; (**f**), $[Co(Bzo_2[18]py_2N_4)]$@NaY; (**g**), $[Co(Bzo_2[20]py_2N_4)]$@NaY

nanocavity is still possible and no unreacted $[Co(N–N)_2]^{2+}$ ions was detected. Furthermore, the spectroscopic data suggest that the encapsulated complex nanoparticle experience very little distortion in the supercage and that the chemical ligation to the zeolite surface is minimal.

Acknowledgment Author is grateful to Council of University of Kashan for providing financial support to undertake this work.

References

1. Corma, A., Diaz-Cabanas, M.J., Jorda, J.L., Martinez, C., Moliner, M.: High throughput synthesis and catalytic properties of a molecular sieve with 18-and 10-member rings. Nature **443**, 842–845 (2006). doi:10.1038/nature05238
2. Tao, Y.S., Kanoh, H., Abrams, L., Kaneko, K.: Mesopore-modified zeolites: preparation, characterization, and applications. Chem. Rev. **106**, 896–910 (2006). doi:10.1021/cr040204o
3. Schüth, F., Schmidt, W.: Microporous and mesoporous materials. Adv. Mater. **14**, 629–638 (2002). doi:10.1002/1521-4095(20020503)14:9<629::AID-ADMA629>3.0.CO;2-B
4. Schüth, F., Sing, K., Weitkamp, J. (eds.): Handbook of Porous Solids, vol. I–V. Wiley-VCH, Weinheim (2002) and references therein
5. Cheetham, A.K., Ferey, G., Loiseau, T.: Open-framework inorganic materials. Angew. Chem. Int. Ed. **38**, 3268–3292 (1999). doi:10.1002/(SICI)1521-3773(19991115)38:22<3268::AID-ANIE3268>3.0.CO;2-U
6. Kaucky, D., Vondrova, A., Dedecek, J., Wichterlova, B.: Activity of Co ion sites in ZSM-5, ferrierite, and mordenite in selective catalytic reduction of NO with methane. J. Catal. **194**, 318–329 (2000). doi:10.1006/jcat.2000.2925
7. Salavati-Niasari, M.: Template synthesis and characterization of host (nanopores of zeolite Y)/guest (Co(II)-tetraoxodithiatetraaza macrocyclic complexes) nanocomposite materials. Polyhedron **27**, 3207–3214 (2008). doi:10.1016/j.poly.2008.07.008
8. Salavati-Niasari, M.: Synthesis, characterization and catalytic oxidation of cyclohexene with molecular oxygen with host (nanopores of zeolite-Y)/guest (Ni(II) complexes of 14- and 16-membered tetraaza dioxo diphenyl macrocyclic ligands) nanocomposite materials. Polyhedron **27**, 3132–3140 (2008). doi:10.1016/j.poly.2008.06.033
9. Hartman, M.: Selective oxidations of linear alkanes with molecular oxygen on molecular sieve catalysts—a breakthrough. Angew. Chem. Int. Ed. **39**, 888–890 (2000). doi:10.1002/(SICI)1521-3773(20000303)39:5<888::AID-ANIE888>3.0.CO;2-R
10. Salavati-Niasari, M.: Oxidation of tetrahydrofuran with hydrogen peroxide in the presence of host (zeolite Y)/guest (1, 9-dialkyl-1, 3, 7, 9, 11, 15-hexaazacyclohexadecane copper(II) complexes, [Cu(R2[16]aneN6)]2+) nanocomposite materials. Inorg. Chem. Commun. **9**, 628–633 (2006). doi:10.1016/j.inoche.2006.03.018
11. Salavati-Niasari, M., Davar, F.: Host (nanodimensional pores of zeolite Y)–guest (3, 10-dialkyl-dibenzo-1, 3, 5, 8, 10, 12-hexaazacyclotetradecane, [Ni(R2Bzo2[14]aneN6)]2+) nanocomposite materials: Synthesis, characterization and catalytic oxidation of cyclohexene. Inorg. Chem. Commun. **9**, 263–268 (2006). doi:10.1016/j.inoche.2005.11.005
12. Salavati-Niasari, M., Davar, F.: Synthesis, characterization and catalytic activity of copper(II) complexes of 14-membered macrocyclic ligand; 3, 10-dialkyl-dibenzo-1, 3, 5, 8, 10, 12-hexaazacyclotetradecanel/zeolite encapsulated nanocomposite materials. Inorg. Chem. Commun. **9**, 304–309 (2006). doi:10.1016/j.inoche.2005.12.006

13. Salavati-Niasari, M.: Host (nanocavity of zeolite-Y)–guest (tetraaza[14]annulene copper(II) complexes) nanocomposite materials: Synthesis, characterization and liquid phase oxidation of benzyl alcohol. J. Mol. Catal. Chem. **245**, 192–199 (2006). doi: 10.1016/j.molcata.2005.09.046
14. Maurya, M.R., Titinchi, S.J.J., Chand, S.: Catalytic activity of chromium(III), iron(III) and bismuth(III) complexes of 1,2-bis(2-hydroxybenzamido)ethane (H2hybe) encapsulated in zeolite-Y for liquid phase hydroxylation of phenol. J. Mol. Catal. Chem. **214**, 257–264 (2004). doi:10.1016/j.molcata.2003.12.017
15. Li, G., Chen, L., Bao, J., Li, T., Mei, F.: A recoverable catalyst Co(salen) in zeolite Y for the synthesis of methyl *N*-phenylcarbamate by oxidative carbonylation of aniline. Appl. Catal. A **346**, 134–139 (2008)
16. Parpot, P., Teixeira, C., Almeida, A.M., Ribeiro, C., Neves, I.C., Fonseca, A.M.: Redox properties of (1-(2-pyridylazo)-2-naphthol) copper(II) encapsulated in Y Zeolite. Microporous Mesoporous Mater. **117**, 297–303 (2009)
17. Fan, B., Li, H., Fan, W., Jin, C., Li, R.: Oxidation of cyclohexane over iron and copper salen complexes simultaneously encapsulated in zeolite Y. Appl. Catal. A **340**, 67–75 (2008)
18. Salavati-Niasari, M.: Nanoscale microreactor-encapsulation of 16-membered hexaaza macrocycle nickel(II) complexes: in situ one-pot template synthesis (IOPTS), characterization and catalytic activity. Microporous Mesoporous Mater. **92**, 173–180 (2006)
19. Salavati-Niasari, M.: Ship-in-a-bottle synthesis, characterization and catalytic oxidation of styrene by host (nanopores of zeolite-Y)/guest ([bis(2-hydroxyanil)acetylacetonato manganese(III)]) nanocomposite materials (HGNM). Microporous Mesoporous Mater. **95**, 248–256 (2006)
20. Salavati-Niasari, M.: Selective oxidation of cyclohexene to di-2-cyclohexenylether by host (nanocavity of zeolite-Y)/guest (manganese(II) complexes with 12- and 14-membered tetraazaz tetraone macrocyclic complexes) nanocomposite materials (HGNM). J. Mol. Catal. A **272**, 249–257 (2007)
21. Salavati-Niasari, M., Sobhani, A.: Ship-in-a-bottle synthesis, characterization and catalytic oxidation of cyclohexane by Host (nanopores of zeolite-Y)/guest (Mn(II), Co(II), Ni(II) and Cu(II) complexes of bis(salicyaldehyde)oxaloyldihydrazone) nanocomposite materials. J. Mol. Catal. A **285**, 58–67 (2008)
22. Salavati-Niasari, M.: Host (nanocavity of zeolite-Y)/guest ([Cu([R]2–N2X2)]2 + (R = H, CH3; X = NH, O, S) nanocomposite materials: Synthesis, characterization and catalytic oxidation of ethylbenzene. J. Mol. Catal. A **284**, 97–107 (2008)
23. Arends, I.W.C.E., Sheldon, R.A.: Activities and stabilities of heterogeneous catalysts in selective liquid phase oxidations: recent developments. Appl. Catal. A **212**, 175–187 (2001)
24. Knops-Gerrits, P.P., Thibault-Starzyk, F., Jacobs, P.A.: Adipic acid synthesis via oxidation of cyclohexene over zeolite occulded manganese diimine complexes. Stud. Surf. Sci. Catal. **84**, 1411–1418 (1994)
25. Balkus Jr., K.J., Khanrnamedova, A.K., Dixon, K.M., Bedioui, F.: Oxidations catalyzed by zeolite ship-in-a-bottle complexes. Appl. Catal. A **143**, 159–173 (1996)
26. Chatterjee, D., Mitr, A.: Olefin epoxidation catalysed by Schiff-base complexes of Mn and Ni in heterogenised-homogeneous systems. J. Mol. Catal. A **144**, 363–367 (1999)
27. Salavati-Niasari, M.: Synthesis and characterization of host (nanodimensional pores of zeolite-Y)–guest [unsaturated 16-membered octaaza–macrocycle manganese(II), cobalt(II), nickel(II), copper(II), and zinc(II) complexes] nanocomposite materials. Chem. Lett. **34**, 1444–1449 (2005)
28. Salavati-Niasari, M.: Nanoscale microreactor-encapsulation 14-membered nickel(II) hexamethyl tetraaza: synthesis, characterization and catalytic activity. J. Mol. Catal. A **229**, 159–164 (2005)
29. Salavati-Niasari, M.: Nanodimensional microreactor-encapsulation of 18-membered decaaza macrocycle copper(II) complexes. Chem. Lett. **34**, 244–249 (2005)
30. McMorn, P., Hutchings, G.J.: Heterogeneous enantioselective catalysts: strategies for the immobilisation of homogeneous catalysts. Chem. Soc. Rev. **33**, 108–122 (2004)
31. Jacob, C.R., Varkey, S.P., Ratnasamy, P.: Zeolite-encapsulated copper (X2-salen) complexes. Appl. Catal. A **168**, 353–364 (1998)
32. Rani, V.R., Kishan, M.R., Kulkarni, S.J., Raghavan, K.V.: Immobilization of metalloporphyrin complexes in molecular sieves and their catalytic activity. Catal. Commun. **6**, 531–538 (2005)
33. Basset, J., Denney, G.H., Jeffery, G.H., Mendham, J.: Vogel's textbook of quantitative inorganic analysis, p. 429. Wiley, New York (1987)
34. Stotz, R.W., Stoufer, R.C.: A novel macrocyclic binuclear copper(II) complex exhibiting a metal–metal interaction. Chem. Commun. 1682–1683 (1970)
35. Salavati-Niasari, M., Shakouri-Arani, M., Davar, F.: Flexible ligand synthesis, characterization and catalytic oxidation of cyclohexane with host (nanocavity of zeolite-Y)/guest (Mn(II), Co(II), Ni(II) and Cu(II) complexes of tetrahydro-salophen) nanocomposite materials. Microporous Mesoporous Mater. **116**, 77–85 (2008)
36. Lineares-Solano, A.: Textural characterization of porous carbons by physical adsorption of gases. In: Figueiredo, J.L., Moulijn, J.A. (eds.) Carbon and Coal Gasification, vol. 137. Martinus Nijho, Dordrecht, MA (1986)
37. Herron, N., Stucky, G.D., Tolman, C.A.: Shape selectivity in hydrocarbon oxidations using zeolite encapsulated iron phthalocyanine catalysts. J. Chem. Soc., Chem. Commun. 1521–1522 (1986)
38. Diegruber, H., Plath, P.J., Schulz-Ekloff, G., Mohl, M.: Study on the structure, stability and propene oxidation capability of faujasite-encaged cobalt chelate complexes. J Mol. Catal. **24**, 115–126 (1984)
39. Salavati-Niasari, M.: Nanoscale microreactor-encapsulation of 18-membered decaaza macrocycle nickel(II) complexes. Inorg. Chem. Commun. **8**, 174–177 (2005)
40. Salavati-Niasari, M.: Zeolite-encapsulated nickel (II) complexes with 14-membered hexaaza macrocycle: synthesis and characterization. Inorg. Chem. Commun. **7**, 963–966 (2004)
41. Sobalik, Z., Dedecek, J., Ikonnikov, I., Wichterlova, B.: State and coordination of metal ions in high silica zeolites Incorporation, development and rearrangement during preparation and catalysis. Microporous Mesoporous Mater. **21**, 525–532 (1998)
42. Abraham, R., Yusuff, K.K.M.: Copper(II) complexes of embelin and 2-aminobenzimidazole encapsulated in zeolite Y-potential as catalysts for reduction of dioxygen. J. Mol. Catal. A **198**, 175–183 (2003)
43. Salavati-Niasari, M.: Host (nanocage of zeolite–Y)/guest (manganese(II), cobalt(II), nickel(II) and copper(II) complexes of 12-membered macrocyclic Schiff-base ligand derived from thiosemicarbazide and glyoxal) nanocomposite materials: Synthesis, characterization and catalytic oxidation of cyclohexene. J. Mol.Catal. A **283**, 120–128 (2008)
44. Nakamoto, K.: Infrared spectra of inorganic and coordination compounds, 2nd edn. Wiley Interscience, New York (1970)
45. Rana, V.B., Gurtu, J.N., Teotia, M.P.: Five and six coordinate complexes of trivalent chromium, manganese and cobalt with tri and tetradentate ligands. J. Inorg. Nucl. Chem. **42**, 331–341 (1980)
46. Rana, V.B., Singh, D.P., Singh, P., Teotia, M.P.: Divalent nickel, cobalt and copper complexes of a tetradentate N_6 macrocyclic ligand. Trans. Met. Chem. **6**, 36–39 (1981)

47. Singh, D.P., Rana, V.B.: Binuclear chromium(III), manganese(III), iron(III) and cobalt(III) complexes bridged by diaminopyridine. Polyhedron **14**, 2901–2906 (1995)
48. Taylor, L.T., Patton, R.D.: Iron(III) complexes of pentadentate ligands. Inorg. Chim. Acta **8**, 191–193 (1974)
49. Rao, C.N.R.: Chemical application of infrared spectroscopy. Academic Press, New York (1963)
50. Adams, D.M.: Metal-ligand and related vibrations. Arnold, London (1967)
51. Ferraro, J.R.: Low frequency vibrations of inorganic and coordination compounds. Plenum Press, New York (1971)
52. Clark, R.J.H., Williams, C.S.: The far-infrared spectra of metal-halide complexes of pyridine and related ligands. Inorg. Chem. **4**, 350–357 (1965)
53. Nakamoto, K.: Infrared spectra of inorganic and coordination compounds. Wiley/Interscience, New York (1970)
54. Lever, A.B.P.: Crystal field spectra, inorganic electronic spectroscopy, 1st edn, p. 249. Elsevier, Amsterdam (1968)
55. Shakir, M., Varkey, S.P., Hameed, P.S.: Divalent, cobalt, nickel, copper and zinc complexes of tetraaza macrocycles bearing polyamide groups: synthesis and characterization. Polyhedron **12**, 2775–2780 (1993)
56. Shakir, M., Nasman, O.S.M., Mohamed, A.K., Varkey, S.P.: N_5, 17, 18-membered pentaazamacrocyclic complexes bearing diamide groups : synthesis and characterization. Ind. J. Chem. **35A**, 710–713 (1996)
57. Athar, F., Arjmand, F., Tabassum, S.: New asymmetric N_2S_2 macrocycles, their metal chelates and the photokinetics of DNA-complex interaction. Trans. Met. Chem. **26**, 426–429 (2001)
58. Mercer, E.E., Buckley, R.R.: Hexaaquoruthenium(II). Inorg. Chem. **4**, 1692–1695 (1981)
59. Pederson, L.A., Lunsford, J.H.: A study of ruthenium in zeolite-Y by X-ray photoelectron spectroscopy. J. Catal. **61**, 39–47 (1980)
60. Briggs, D., Seah, M.P. (eds.): Practical Surface Analysis. Wiley, New York (1980)